Supplement to the article:
Late Pleistocene Aggradation and Holocene Surface Reworking of Fluvial Terraces in the glacially overprinted Western Higher Himalaya

Jonas Kordt[1], Saptarshi Dey[2], Bodo Bookhagen[3], Georg Rugel[4], Johannes Lachner[4], Carlos Vivo-Vilches[4,5], Naveen Chauhan[6], Rasmus Thiede[1]

[1]Institute of Geosciences, Kiel University, Kiel, 24118, Germany
[2]Department of Geology and Geophysics, Indian Institute of Technology Kharagpur, 721302, India
[3]Institute of Geosciences, University of Potsdam, Potsdam, 14476, Germany
[4]Institute of Ion Beam Physics and Materials Research, Helmholtz-Zentrum Dresden-Rossendorf, Dresden, 01328, Germany
[5]Faculty of Physics, University of Vienna, Vienna, 1090, Austria
[6]Physical Research Laboratory, Ahmedabad, 380009, India

Correspondence to: Jonas Kordt (jonas.kordt@ifg.uni-kiel.de)

Supplement Figures and Tables

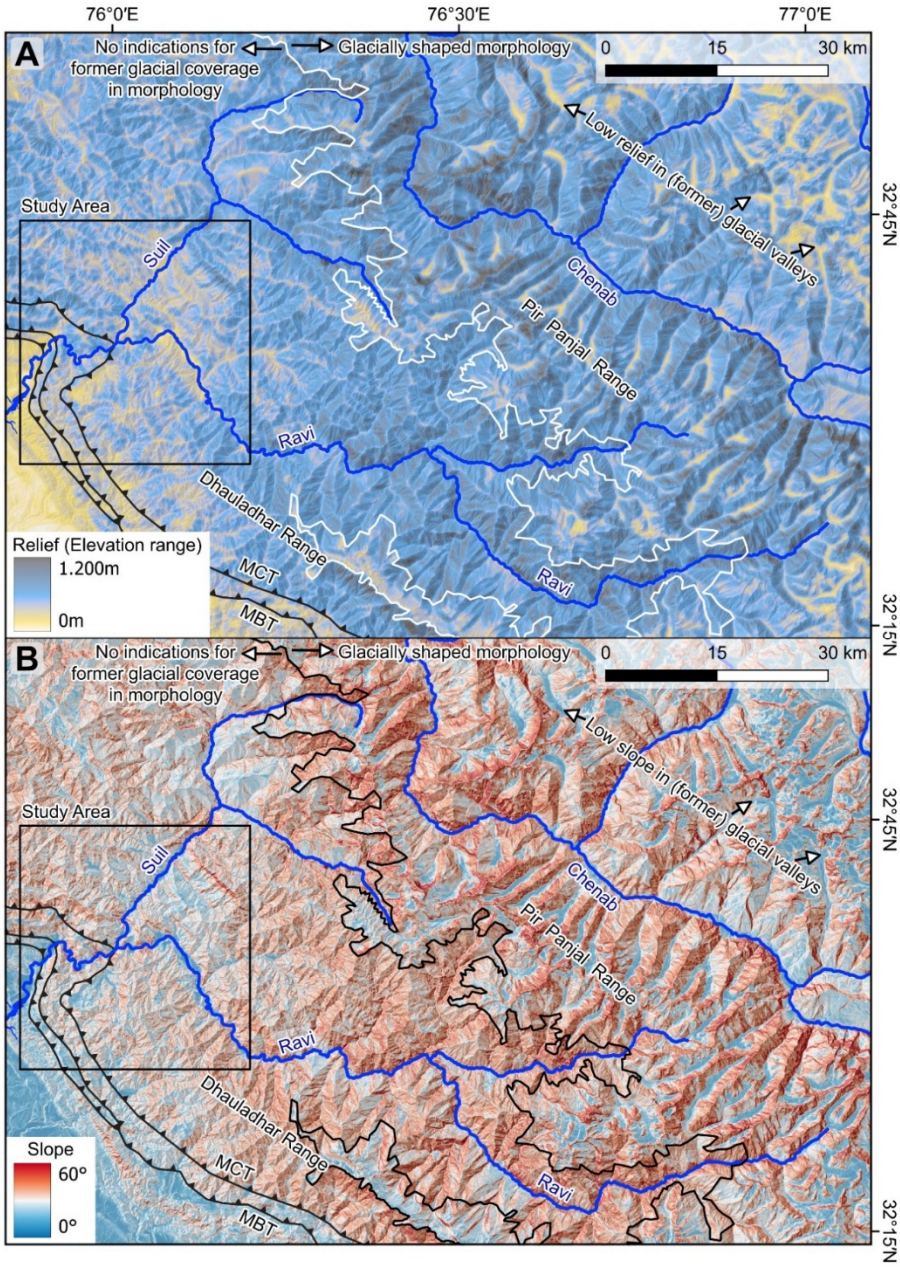

Figure S1: A: 500-m radius topographic relief map and **B**: Slope map of the study area and the Ravi and Suil headwaters showing potential past glacial coverage. The boundary between glacially and non-glacially shaped morphology was mapped by using multiple terrain attributes (topography, roughness, relief), satellite imagery, field observations in the Ravi Region, and findings of traverses through the area conducted while sampling rocks used for thermochronologic dating (Deeken et al., 2011). It should be noted that this does not indicate continuous glacial coverage across the entire area, as numerous valleys, especially along steep upper mountain flanks, lack evidence for former glaciation. Both maps show that our study area is less steep and has a lower relief than the headwaters of the Ravi and Suil, which enables the preservation of river terraces along both rivers. DEM by JAXA (AW3D30).

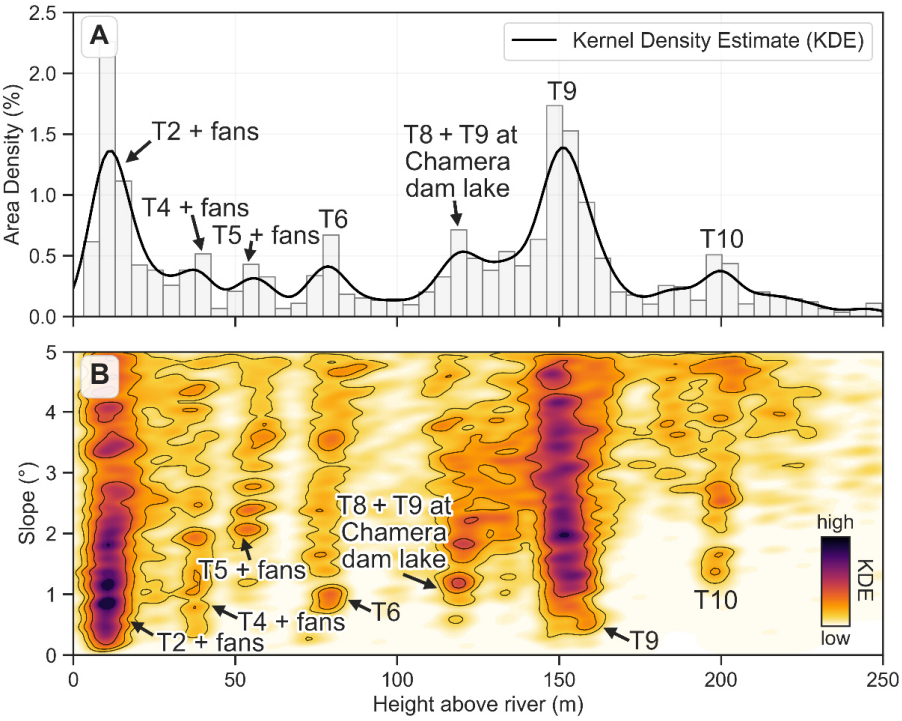

Figure S2: Combined Histogram and Kernel Density Estimate (KDE) plot showing the widespread terrace levels along the studied Ravi and Suil River sections (cf. Fig. 3 in the main manuscript). In contrast to Fig. 5 (in the main manuscript) we only use the digital elevation data of all preselected terraces shown in Fig. 3 (in the main manuscript). We furthermore filter the elevation model (Resolution: 30 m) data to heights up to 250 meters where the slope of the model cell is ≤ 5°. **A**: Histogram of the filtered height values showing their distribution over height as area density in percent. For the KDE we used a bandwidth of 0.2. **B**: KDE plot based on the same filtered height values, but now plotted as height against slope using a bandwidth of 0.4. Darker colours show a higher density estimate of the area. Please note that tributary fans are also included in the lower levels mostly up to T5. Below the T9 level (120-140 m) are some terrace surfaces shown with heights that are impacted by the sedimentation related to the Chamera dam. These heights are lower than T9, although this is the same terrace level.

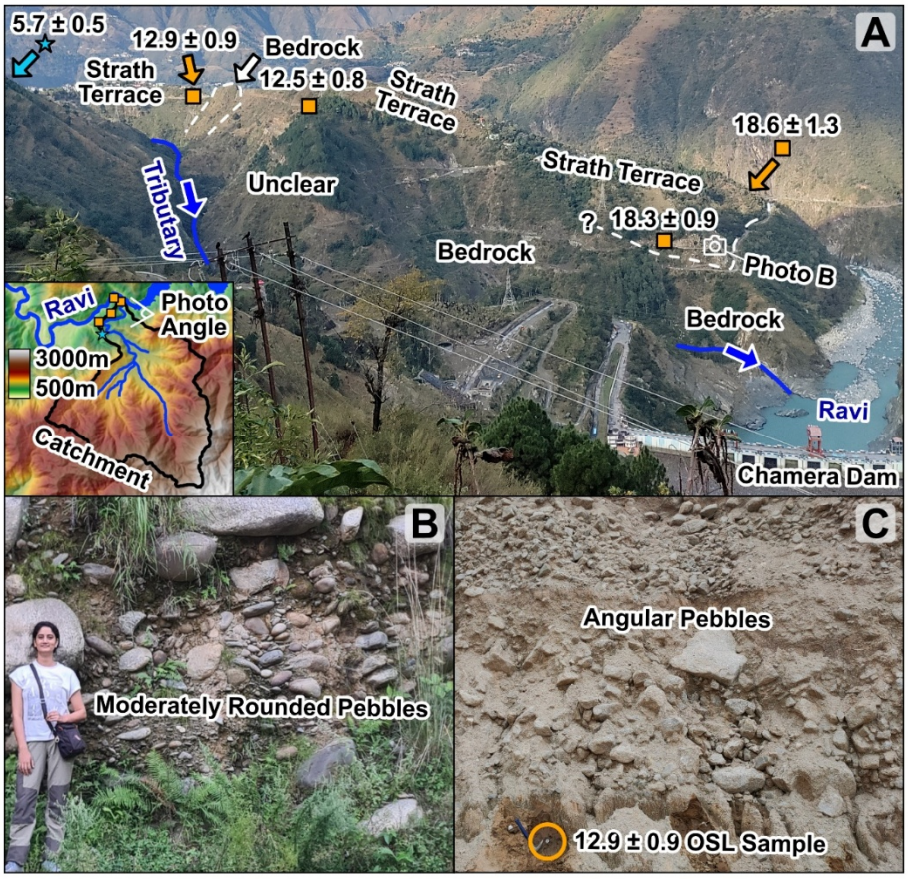

Figure S3: Photos of the isolated ~300 – 350 m high terrace in the Ravi River catchment west of the Chamera Dam. **A**: Terrace overview with all age datings. Optically stimulated luminescence (OSL) ages are shown with orange squares, while the ^{10}Be age is represented by a blue star. Arrows indicate sample locations, when they are not within the picture. White dotted line shows the border between bedrock and terrace material. As most sections were not accessible the exact border is not clear and therefore not drawn for most sections. Inset shows digital elevation model off the tributary catchment including sample and Photo locations. DEM by JAXA (AW3D30). **B**: Detail photo of the fluvial material close above the bedrock, which we dated to ~18 – 19 ky using OSL. **C**: Detail section of the material near the terrace top where the 12.9 ± 0.9 ky OSL sample was taken. In contrast to the material in (B), all pebbles are angular and mostly made up of Gneiss from the Dhauladhar Range.

Sample Name	0 mm/ky ^{10}Be Age (ky)	0 mm/ky ^{26}Al Age (ky)	5 mm/ky ^{10}Be Age (ky)	5 mm/ky ^{26}Al Age (ky)	10 mm/ky ^{10}Be Age (ky)	10 mm/ky ^{26}Al Age (ky)	20 mm/ky ^{10}Be Age (ky)	20 mm/ky ^{26}Al Age (ky)	40 mm/ky ^{10}Be Age (ky)	40 mm/ky ^{26}Al Age (ky)
NWR21-41	4.8 ± 0.4	5.9 ± 0.8	4.9 ± 0.4	6.1 ± 0.9	5.0 ± 0.4	6.2 ± 0.9	5.3 ± 0.5	6.5 ± 1.0	5.7 ± 0.6	7.3 ± 1.3
NWR21-43	2.5 ± 0.3	2.6 ± 0.4	2.6 ± 0.3	2.6 ± 0.4	2.6 ± 0.3	2.6 ± 0.4	2.6 ± 0.3	2.7 ± 0.4	2.7 ± 0.4	2.8 ± 0.5
NWR21-46	5.6 ± 0.6	6.0 ± 0.7	5.7 ± 0.6	6.1 ± 0.7	5.9 ± 0.6	6.3 ± 0.8	6.2 ± 0.7	6.6 ± 0.8	6.9 ± 0.9	7.4 ± 1.1
NWR21-48	5.3 ± 0.5	5.1 ± 0.9	5.4 ± 0.6	5.2 ± 0.9	5.5 ± 0.6	5.3 ± 1.0	5.7 ± 0.6	5.5 ± 1.1	6.4 ± 0.8	6.0 ± 1.3
NWR21-50	7.3 ± 0.6	8.1 ± 1.4	7.4 ± 0.7	8.4 ± 1.5	7.6 ± 0.7	8.7 ± 1.6	8.2 ± 0.8	9.6 ± 1.9	9.8 ± 1.2	11.3 ± 2.8
NWR21-52	2.7 ± 0.3	2.4 ± 0.4	2.8 ± 0.3	2.4 ± 0.5	2.8 ± 0.3	2.4 ± 0.5	2.8 ± 0.3	2.5 ± 0.5	3.0 ± 0.4	2.6 ± 0.5
NWR21-53	6.0 ± 0.6	6.2 ± 0.8	6.1 ± 0.7	6.4 ± 0.8	6.3 ± 0.7	6.5 ± 0.9	6.6 ± 0.8	6.8 ± 1.0	7.3 ± 1.0	7.6 ± 1.2
SD17CRN02	15.4 ± 1.3	11.9 ± 1.3	16.5 ± 1.5	12.5 ± 1.4	17.7 ± 1.8	13.0 ± 1.5	21.0 ± 2.6	14.5 ± 2.0	0.0 ± 0.0	20.7 ± 4.7
SD17CRN12	5.6 ± 0.6	5.6 ± 0.6	5.7 ± 0.6	5.7 ± 0.7	5.9 ± 0.6	5.8 ± 0.7	6.2 ± 0.7	6.1 ± 0.8	6.9 ± 0.9	6.8 ± 1.0
SD17CRN14	1.8 ± 0.6	1.8 ± 1.1	1.8 ± 0.6	1.8 ± 1.1	1.8 ± 0.6	1.8 ± 1.1	1.8 ± 0.7	1.9 ± 1.1	1.9 ± 0.7	1.9 ± 1.2
SD17CRN16	1.7 ± 0.6	1.6 ± 1.0	1.8 ± 0.6	1.6 ± 1.0	1.8 ± 0.6	1.6 ± 1.0	1.8 ± 0.6	1.7 ± 1.0	1.9 ± 0.6	1.7 ± 1.1
SD17CRN17	2.4 ± 0.5		2.4 ± 0.5		2.5 ± 0.5		2.5 ± 0.5		2.6 ± 0.6	
JK-22-09	3.1 ± 0.5	2.0 ± 1.0	3.1 ± 0.5	2.0 ± 1.0	3.1 ± 0.5	2.1 ± 1.0	3.2 ± 0.5	2.1 ± 1.1	3.4 ± 0.6	2.2 ± 1.1
JK-22-12	7.0 ± 0.8	5.5 ± 1.2	7.2 ± 0.9	5.6 ± 1.2	7.4 ± 0.9	5.7 ± 1.3	7.9 ± 1.0	6.0 ± 1.4	9.4 ± 1.5	6.7 ± 1.8
JK-22-14	5.8 ± 0.6		5.9 ± 0.7		6.1 ± 0.7		6.4 ± 0.8		7.1 ± 1.0	
JK-22-15	3.2 ± 0.7		3.2 ± 0.7		3.3 ± 0.7		3.4 ± 0.7		3.6 ± 0.8	
JK-22-16	4.0 ± 0.5		4.1 ± 0.5		4.1 ± 0.5		4.3 ± 0.5		4.6 ± 0.6	
JK-22-17	3.8 ± 1.2	3.5 ± 0.6	3.8 ± 1.3	3.5 ± 0.6	3.9 ± 1.3	3.6 ± 0.6	4.0 ± 1.4	3.7 ± 0.7	4.3 ± 1.6	4.0 ± 0.8
JK-22-20	3.3 ± 0.6	4.2 ± 1.1	3.3 ± 0.6	4.2 ± 1.2	3.4 ± 0.7	4.3 ± 1.2	3.5 ± 0.7	4.5 ± 1.3	3.7 ± 0.8	4.9 ± 1.5
JK-22-21	6.5 ± 0.7	6.5 ± 2.5	6.6 ± 0.8	6.7 ± 2.7	6.8 ± 0.8	6.8 ± 2.8	7.1 ± 0.9	7.2 ± 3.2	8.1 ± 1.2	8.2 ± 4.2
JK-22-23	5.6 ± 0.6	6.9 ± 0.8	5.7 ± 0.6	7.0 ± 0.9	5.9 ± 0.6	7.2 ± 0.9	6.2 ± 0.7	7.6 ± 1.1	6.9 ± 0.8	9.0 ± 1.5
JK-22-24	3.7 ± 0.4	2.3 ± 0.5	3.8 ± 0.4	2.3 ± 0.6	3.8 ± 0.5	2.4 ± 0.6	4.0 ± 0.5	2.4 ± 0.6	4.2 ± 0.6	2.5 ± 0.6
JK-22-25	4.8 ± 0.5	5.7 ± 2.6	4.9 ± 0.5	5.8 ± 2.7	5.0 ± 0.5	6.0 ± 2.9	5.2 ± 0.6	6.3 ± 3.2	5.7 ± 0.7	7.0 ± 4.1
JK-22-26	4.2 ± 0.4	2.7 ± 0.8	4.3 ± 0.4	2.8 ± 0.8	4.4 ± 0.4	2.8 ± 0.9	4.5 ± 0.4	2.9 ± 0.9	5.0 ± 0.5	3.0 ± 1.0
JK-22-27	2.0 ± 0.3		2.0 ± 0.3		2.0 ± 0.3		2.1 ± 0.3		2.2 ± 0.3	
JK-22-28	2.3 ± 0.3	2.2 ± 0.7	2.4 ± 0.3	2.2 ± 0.7	2.4 ± 0.3	2.2 ± 0.7	2.5 ± 0.3	2.3 ± 0.8	2.6 ± 0.3	2.4 ± 0.8
JK-22-33	6.2 ± 0.5		6.4 ± 0.5		6.5 ± 0.6		6.9 ± 0.6		7.7 ± 0.8	
JK-22-36	10.3 ± 0.9	9.0 ± 1.4	10.8 ± 1.0	9.4 ± 1.5	11.2 ± 1.1	9.8 ± 1.7	12.1 ± 1.3	10.5 ± 2.0	15.2 ± 2.3	12.5 ± 3.0
JK-22-40	5.0 ± 0.4	4.4 ± 1.7	5.2 ± 0.4	4.5 ± 1.8	5.3 ± 0.4	4.5 ± 1.8	5.5 ± 0.5	4.7 ± 2.0	6.0 ± 0.6	5.2 ± 2.4
JK-22-42	6.0 ± 0.4	4.1 ± 0.6	6.2 ± 0.4	4.2 ± 0.6	6.3 ± 0.5	4.2 ± 0.6	6.7 ± 0.5	4.4 ± 0.7	7.4 ± 0.7	4.7 ± 0.8
JK-22-43	4.4 ± 0.3	4.4 ± 1.1	4.5 ± 0.3	4.5 ± 1.2	4.6 ± 0.4	4.5 ± 1.2	4.8 ± 0.4	4.7 ± 1.3	5.3 ± 0.5	5.2 ± 1.6
JK-22-46	4.1 ± 0.3		4.1 ± 0.3		4.2 ± 0.4		4.3 ± 0.4		4.7 ± 0.5	
JK-22-48	4.3 ± 0.4	4.5 ± 1.5	4.4 ± 0.4	4.6 ± 1.6	4.5 ± 0.4	4.7 ± 1.7	4.7 ± 0.4	4.9 ± 1.8	5.2 ± 0.5	5.4 ± 2.2
JK-22-49	5.2 ± 0.4	4.2 ± 0.6	5.3 ± 0.4	4.3 ± 0.6	5.4 ± 0.4	4.3 ± 0.6	5.7 ± 0.5	4.5 ± 0.7	6.3 ± 0.6	4.9 ± 0.8
JK-22-51	4.6 ± 0.4		4.6 ± 0.4		4.7 ± 0.4		5.0 ± 0.5		5.4 ± 0.6	
JK-22-59	5.7 ± 0.5	7.0 ± 3.4	5.8 ± 0.6	7.2 ± 3.6	5.9 ± 0.6	7.3 ± 3.8	6.2 ± 0.7	7.8 ± 4.3	6.9 ± 0.8	9.2 ± 6.1

Table S1: Cosmogenic surface exposure ages for ^{10}Be and ^{26}Al with different erosion rates. Please note, that due to the young ages the differences between different erosion rates are small for most samples. ^{26}Al results with an underscore have a low measurement output, which we consider unreliable. For details about the calculation see Section 3.1.

Supplement Text 1: Activities within a tributary catchment near Chamera Dam

In addition to the 10 main terrace levels in the main manuscript, we also identified an isolated terrace at the junction of a local tributary with the Ravi River directly downstream of the Chamera dam, where a bedrock terrace with a veneer of gravels (strath terrace) rises from ~80 m to ~300 – 350 m above the present Ravi River valley bottom (Fig. 3D in the main manuscript). In contrast to other terraces, the height of the exposed bedrock above the river varies strongly along this terrace, from ~80 m up to ~330 m at the top in some sections (Fig. S3A). Our two new optically stimulated luminescence (OSL) Ages with ~18 ky, taken slightly above the bedrock terrace contact, correspond well with a third age from near the surface of the T7 terrace. The dated lower terrace material is medium- to well-rounded and has the same lithologies present within other Ravi terraces (Fig. S3B). We therefore interpret this material as deposited by the Ravi during the same time as the upper part of the T7 terrace. The material above, however, on the same isolated terrace, is different and nearly all pebbles are angular, and there is a higher abundance of local gneiss from the Dhauladhar Range (Fig. S3C). The two obtained near-surface luminescence ages of this upper material are both ~13 ky (Fig. 7, Profile 3 in the main manuscript and Fig. S3A). This suggests that after deposition of the lower terrace, one or multiple events, affecting only the tributary catchment, deposited the material on the lower part. We note that the height and ages of the upper terrace part do not correspond with the near-surface ages of the 100 m lower T10 level in the study area, which is more than ~3 times as old (Joshi et al., 2022). The height of this terrace is therefore not in balance with other terraces upstream and downstream at the Ravi River, which indicates that the upper part of this geomorphic feature was not adjusted or in equilibrium with the base level of the Ravi River during the time of deposition and formation. Because the terrace is multiple kilometres away from steep hillslopes and the surface exhibits a strong curvature, surface processes affecting other terraces (e.g., landslides) are not expected on this terrace. We therefore interpret the near-surface OSL ages to reflect the local deposition of tributary material forming this unique terrace surface, rather than the basin-wide aggradation of Ravi River pebbles during the Late Pleistocene. Future work is needed to reconstruct the reasons behind the past disequilibrium of the tributary with the Ravi catchment.

References

Deeken, A., Thiede, R. C., Sobel, E. R., Hourigan, J. K., and Strecker, M. R.: Exhumational variability within the Himalaya of northwest India, Earth and Planetary Science Letters, 305, 103–114, https://doi.org/10.1016/j.epsl.2011.02.045, 2011.

Joshi, M., Thakur, V. C., Suresh, N., and Sundriyal, Y. P.: Climate-tectonic imprints on the Late Quaternary Ravi River Valley Terraces of the Chamba region in the NW Himalaya, Journal of Asian Earth Sciences, 223, 104990, https://doi.org/10.1016/j.jseaes.2021.104990, 2022.